Bonding and Correlation Analysis of Various SiCO Isomers

Yuxiang Bu*,†,‡,§ and Keli Han†

Institute of Theoretical Chemistry, Shandong University, Jinan, 250100 P. R. China, State Key Laboratory of Molecular Reaction Dynamics, Dalian Institute of Chemical Physics, Dalian, 116023 P. R. China, and Department of Chemistry, Qufu Normal University, Qufu, 273165 P. R. China

Received: June 6, 2002; In Final Form: October 8, 2002

The structural properties for various SiCO isomers in the singlet and triplet states have been investigated using CASSCF methods with a 6-311+G* basis set and also using three DFT and MP2 with same basis set for those systems except for the linear singlet state. The detailed bonding character is discussed, and the state−state correlations and the isomerization mechanism are also determined. Results indicate that there are four different isomers for each spin state, and for all isomers, the triplet state is more stable than the corresponding singlet state. The most stable is the linear SiCO ($^3\Sigma^-$) species and may be referred to the ground state. At the CASSCF-MP2(full)/6-311+G* level, the state−state energy separations of the other triplet states relative to the ground state are 43.2 (cyclic), 45.2 (linear SiOC), and 75.6 kcal/mol (linear CSiO), respectively, whereas the triplet−singlet state excitation energies for each configuration are 17.3 (linear SiCO), 2.2 (cyclic SiCO), 10.2 (linear SiOC), and 18.5 kcal/mol (linear CSiO), respectively. SiCO ($^3\Sigma^-$) may be classified as silene (carbonylsilene), and its $CO^{\delta-}$ moiety possesses CO^- property. The dissociation energy of the ground state is 42.5 kcal/mol at the CASSCF-MP2(full)/6-311+G* level and falls within a range of 36.5−41.5 kcal/mol at DFT level, and of 23.7−28.9 kcal/mol at the wave function-correlated level, whereas the vertical IP is 188.8 kcal/mol at the CASSCF-MP2(full)/6-311+G* level and is very close to the first IP of Si atom. Three linear isomers (SiCO, SiOC, and CSiO) have similar structural bonding character. SiOC may be referred to the iso-carbonyl Si instead of the aether compound, whereas the CSiO isomer may be considered as the combination of C (the analogue of Si) with SiO (the analogue of CO). The bonding is weak for all linear species, and the corresponding potential energy surfaces are flat, and thus these linear molecules are facile. Another important isomer is of cyclic structure, it may be considered as the combination of CO with Si by the side π bond. This structure has the smallest triplet state−singlet state excitation energy (∼2.2 kcal/mol); the C−O bonds are longer, and the corresponding vibrational frequencies are significantly smaller than those of the other linear species. This cyclic species is not classified as an epoxy compound. State−state correlation analysis and the isomerization pathway searches have indicated that there are no direct correlations among three linear structures for each spin state, but they may interchange by experiencing two transition states and one cyclic intermediate. The easiest pathway is to break the Si−O bond to go to the linear SiCO, but its inverse process is very difficult. The most difficult process is to break the C−O bond and to go to the linear CSiO.

1. Introduction

Because of the importance in industry and biological process, the investigations concerning the interaction of carbon suboxides with the functional biological and materials molecules have been the subject in both the theoretical and experimental aspects. In particular, for the studies on the CO species, much important information has been obtained. A recent survey of the stretching frequencies of CO bonded to the biological molecules has shown that there is an interesting change in the vibrational frequency for CO,[1] the affecting factors resulting in the frequency shift mainly involve the ring-ligand substituents,[2] CO ligand binding geometry and steric effects,[3−5] redox potentials,[6] CO binding affinities,[7] and the charge and polar interactions in the protein pocket.[1,8,9] To interpret the dependence of the CO binding on these effect factors, many interesting models have been established. Obviously, the combination of CO with the metalloporphyrins, the heme proteins, and the other complexes with biological functionality may lead to the changes of not only the structural properties of CO but also the biological functionality of the biological molecules. On the other hand, CO is also the pervasive surface adsorbate; it is easily absorbed over the isolated transition metal clusters, the polynuclear transition metal complexes, and the transition metal surfaces, perhaps changing the surface structural properties of materials molecules. Therefore, the detailed investigations regarding the interaction between CO and various clusters and compounds are very interesting for the approaches to the functionality and its control mechanism of the biological and materials molecules.

However, although a series of new progresses have been made, the interaction details and nature between CO and various functional complexes are still unknown, especially for the interaction with nontransition metal and nonmetal clusters, compounds, and the polar molecules, and relevant studies have appeared to be seriously absent. Obviously, the continuous

* To whom correspondence should be addressed.
† Dalian Institute of Chemical Physics.
‡ Shandong University.
§ Qufu Normal University.

10.1021/jp021357n CCC: $22.00
Published on Web 11/15/2002

increase attention on these kinds of irregular bonding interaction studies have indicated that it is very important to study these kinds of slight-weakly bound systems for the investigations of the interaction between CO and the nonmetal-centered active sites in the biological and materials large molecules.

Because of the lack of the bonding active d-orbitals, it can be predicted that when interacting with CO, the nonmetal and nontransition metal atoms will behave with a different character from the transition metals. Perhaps it essentially cannot form polycarbonyl complexes although CO has strong donor−acceptor ability. The binding of the weakly polar CO molecule to alkali metals and the nonmetals has not been studied extensively. To our knowledge, only a few theoretical studies on such kinds of systems have been reported. Early calculations on the Li^+-CO potential energy surface (PES) were carried out by Sraemmler.[10] The X^+-CO (X = H, Li, Na, and K) bond dissociation energies were calculated by Ikuta.[11] More extensive basis sets were used to study the lithium and sodium action affinities of CO by Dixon et al.[12] Walter et al. performed experimental determinations for the sequential bond energies of the $M^+(CO)_n$ (n = 1 or 2 or 3; M = Li, Na, and K).[13] Especially in recent years, some increasing attentions have been paid on the investigations regarding the interactions of CO with alkali metals and the nontransition metals.[14−29] The electronic structures and relevant properties have been investigated in detail using different theoretical methods for Li carbonyls (Li_2-CO,[14] LiC_2O_2,[15] and $Li(CO)_n$ (n = 1, 2, and 3)[16]), Na and K carbonyls, Al carbonyls (AlCO and $Al(CO)_2$)[17−20] and its isocarbonyls (AlOC) and the AlCO cyclic structure,[18,20] etc., and much valuable information has been provided for the further investigations regarding other nontransition metal carbonyls. However, the studies on the nonmetal carbonyl complexes have been found to be absent. Only a part of the subcarbonyl complexes have been experimentally detected by different groups[21−27] for $AsCO^-$, AsCO,[21] $SiCO^-$, $GeCO^-$,[22] BCO, $(BCO)_2$, $B(CO)_2$,[23] SCO,[24,25] CCO,[26,27] and $Si(CO)_n$ (n = 1 and 2),[28,29] but no detailed theoretical reports have been given on the studies of their various properties.

The most detailed investigations for these nonmetal carbonyls should be that of Si carbonyls. In 1977, the Weltner group first reported an experimental detection of the single and double carbonyl Si complexes (SiCO and $Si(CO)_2$) under the cryogenic condition and also used the corresponding electron spin resonance and optical spectra to confirm the existence of these two species.[28] Later, Stolvik further experimentally determined the SiCO molecular structure.[29] Although they claimed that SiCO and $Si(CO)_2$ were linear molecules, they also implied the existence of the bent structures for SiCO with some uncertainty. However, their further semiempirical quantum chemistry CNDO calculations for the SiCO molecule gave some information regarding the unstability of the nonlinear SiCO structure.[28] A reasonable interpretation for this interference is that the molecular bending force constant is quite low, and some constraints in the matrix sites induce bending. Similarly, the structure of $Si(CO)_2$ species being a linear is also doubtable, because there were no certain experimental information for supporting this claim. Our recent theoretical studies on stability of the Si carbonyl complexes have indicated $Si(CO)_2$ species to be a v-type ground-state structure. Another important contribution to the study of Si carbonyls should be referred to the Schaefer group works.[30−33] Using coupled-cluster with single and double excitations (CCSD), configuration interaction with single and double excitations (CISD), and many triple-ζ basis sets, they investigated systematically the electronic structural characterization of silaketenylidene SiCO (carbonylsilene) and 2-silaketenylidene CSiO for their $^3\Sigma^-$ and $^3\Pi$ states, and indicated that there is obviously a Renner-Teller effect only for the linear $^3\Pi$ state. They also reassigned the structure of dicarbonyl Si ($Si(CO)_2$) on the basis of theoretically predicted infrared spectra. Obviously, these studies have provided much valuable information for the further investigation regarding the nontransition metal carbonyls. Because of the lack of bonding active d-orbitals, it may be predicted that it is difficult to form the polycarbonyls. Obviously, these recent works have focused on the triplet ground state ($^3\Sigma^-$) and the first triplet excited state ($^3\Pi$) for the linear SiCO and CSiO species, but no studies have been given for their singlet state isomers. On the other hand, because the CO molecule has two bare π-bond electrons and the lone-pair electrons at the O-end, there also should be the cyclic SiCO and the linear iso-carbonyl SiOC species at both singlet and triplet states. In addition, the theoretical approaches to the relative stability and the state-state isomerization mechanism among several possible SiCO isomers at different low-lying electronic states have also not appeared. In fact, Si cannot use its empty d orbitals to accept the σ-coordination lone electron pair coming from the CO and at the same time use their occupied d-orbitals to interact with empty π^*-antibonding orbitals and to feedback the electron to CO because of the great energy level difference between π^* and the full-empty or fully occupied d orbitals of the nontransition metals and nonmetals. Therefore, it may be predicted that the bonding interaction between CO and nontransition metals is significantly different from that between CO and the transition metals. It should be noted that the density functional theory (DFT) has recently emerged to be a reliable and computationally inexpensive method capable of successfully predicting the properties for many systems[34−39] and, thus, can be desirable to be applied to the calculations on these systems. However, for the possible linear structures of this system, they may exhibit as multireference character and must be described by many determinant wave functions; thus, the complete active space SCF (CASSCF) method may be used for these special systems.

In view of the absence mentioned above, a detailed theoretical investigation will be given for the geometrical parameters, the harmonic frequencies, the dissociation energies, the ionization potentials, and other relevant properties of several [Si,C,O] isomers at the singlet and the triplet states, using CASSCF, DFT, and the wave function-correlated ab initio methods with a relatively large one-particle basis set. The main objective is to accurately predict the geometries and the relevant quantities, to compare the calculated frequencies with the experimental findings, and to explore the state−state correlations and the isomerization mechanism among several isomers at both states.

2. Calculational Details

For the [Si,C,O] system, preliminary theoretical analyses have indicated that because all isomers may present the π^2 configuration, this configuration may generate one $^3\Sigma^-$, one $^1\Delta$, and one $^1\Sigma^+$ when molecules are linear. The $^3\Sigma^-$ state may be described by an open-shell triplet single determinant reference wave function, but two singlet states require at least two determinants to describe them for which, in multireference space self-consist-field calculation, the first root is referred to the $^1\Delta$ state and the second one is referred to the $^1\Sigma^+$ state. Obviously, all DFT and wave function-correlated single determinant ab initio methods (such as MPn, n = 2, 3, 4, CCSD, QCISD, etc.) could not be suitable to treat the linear singlet state systems with $^1\Delta$ or $^1\Sigma^+$ symmetries. Therefore, with a relative large

modest 6-311+G* basis set, the complete active space self-consistent field (CASSCF) method has been first used for the optimizations of various possible [Si,C,O] isomers at both triplet and singlet states. To confirm the calculated results, DFT and the second-order Møller−Plesset perturbation theory (MP2) methods have also been used for the species at triplet state and the nonlinear singlet state.

However, for the linear singlet state, the preliminary analysis indicates that there are three different electron occupations, $(\pi_x)^2$, $(\pi_y)^2$, or $^1(\pi_x{}^1\pi_y{}^1)$, which denote the basis of the multireference space. The $^1\Delta$ state has two basis vectors, $(\pi_x)^2 - (\pi_y)^2$ and $^1(\pi_x{}^1\pi_y{}^1)$, and the $^1\Sigma^+$ has one basis, $(\pi_x)^2 + (\pi_y)^2$. When bending, $^1\Delta$ will split to 1 ^{1}A′ (from $(\pi_x)^2 - (\pi_y)^2$) and 1 ^{1}A″ (from $^1(\pi_x{}^1\pi_y{}^1)$) and $^1\Sigma^+$ will be reduced to 2 ^{1}A′ (from $(\pi_x)^2 + (\pi_y)^2$). In the multireference space calculations, the component $(\pi_x)^2 - (\pi_y)^2$ of the $^1\Delta$ state corresponds to the first root, whereas the basis vector $((\pi_x)^2 + (\pi_y)^2)$ of $^1\Sigma^+$ state corresponds to the second root. Taking as the approximate results, the linear $^1\Delta$ state may be also estimated by approaching from the bent initial geometry with the ^{1}A′ symmetry constraint. Thus, all linear $^1\Delta$ state species are also investigated approximately using DFT and MP2 methods for the approximate comparisons with other systems.

The corresponding three density functionals used are B3LYP, B3P86, and B3PW91, as implemented in Gaussian 94.[40] These three models combine Becke three-parameter hybrid functional, which is a linear combination of Hartree−Fock exchange, Slater exchange, and B88 gradient-corrected exchange[41] with the correlation functionals of Lee, Yang, and Parr,[42,43] Perdew (P86),[44,45] and Perdew and Wang (PW91),[46] respectively. For the complete active space method, the used active space is (4,6), viz., 4 active electrons and 6 active orbitals are included in the complete active space of interest. First, a prior run for single-point calculation with much orbital coefficient information has been used to quickly determine the orbital symmetries and then selects all orbitals which involve the electrons of interest and that they are correlated correctly. Actually, all states of interest considered here originate from the different occupations of two degenerate π orbitals which are the frontier orbitals for two π electrons. So it is enough to design an active space with 6 orbitals and 4 electrons, CAS(4,6), and these active orbitals are (4σ, $2\pi^+$, $2\pi^-$, 5σ, $3\pi^+$, $3\pi^-$) for the linear molecules and ($5a'$, $6a'$, $2a''$, $7a'$, $3a''$, $8a'$) for the bent molecules. At this level, the first roots for every system are searched which just correspond to the states of interest. They are $^3\Sigma^-$ for the linear triplet states, $^1\Delta$ for the linear singlet states, and ^{3}A″ and ^{1}A′ for bent species, respectively.

The geometries are first optimized using the CASSCF(4,6) method described above. The harmonic vibrational frequencies are then obtained from analytic second derivative methods. To compare the optimized results with other suitable methods, the geometries are reoptimized by using DFT and MP2 methods for all linear triplet states and bent molecules, and the harmonic vibrational frequencies are calculated via the analytic gradient and the finite differences of analytic gradients, respectively. As the approximate results, the linear $^1\Delta$ states are estimated from the low symmetric ^{1}A′ state of the quasi-linear molecule. To improve the energy accuracy, single-point calculations have also been done. For the energy determinations of all systems, the CASSCF(4,6)-MP2(full) method with 6-311+G* basis set is used for a MP2-level electron correlation correction to the CASSCF energies. At the same time, the corresponding energy quantities are also calculated at MP2 geometries using the fourth-order Møller−Plesset theory (MP4) with all substitutions and CCSD(T) for some systems. The calculations are performed with the Gaussian 94 program package,[40] and all electrons are included in the electron correlation correction of the relevant energy quantities. For all open-shell systems, the one used is the unrestricted open-shell SCF method in the corresponding optimizations and calculations.

The calculations are mainly limited to the lowest-lying singlet and the lowest-lying triplet states of these isomer species for the structural property and bonding analysis. The dissociation energies (D_e) and the ionization potentials (IP) are then obtained by comparing the energy differences between the ground state and the corresponding dissociated species (Si (^{3}P) + CO($^1\Sigma^+$)) and those between the ground state and the corresponding monovalent cation $SiCO^+$ ($^2\Pi$), respectively.

To find the correlations among all isomers and the state−state isomerization mechanism, the transition state searches have also been performed using the B3LYP/6-311+G* method for the triplet state correlation and the singlet state correlation, respectively. The minimum-energy pathways have been determined for the isomerizations by the internal reaction coordinate scheme and have also been confirmed by scanning the relaxed PES. Because of the good performance of DFT methods and the difficulties in optimizations by wave function-correlated correction methods, the energy correction is also performed at CASSCF(4,6)-MP2(full)/6-311+G* level by using B3LYP/6-311+G* geometries.

Because the accuracy of DFT calculations also depends on the number of points used in the numerical integration, more fine grids should be employed. However, for the comparison of the relative stability of the systems or the computations on the energy differences, the dissociation energy and so on, it is very important to use the same integration point numbers (same grid) for all calculations. Thus, in all DFT calculations performed here, the numerical integration of the functionals are carried out using the Gaussian 94 default grid consisting of 75 radical shells and 302 angular points per shell, resulting in about 7000 points per atoms.

3. Results and Discussions

The geometry optimizations are first performed for various possible combinations [Si,C,O] at singlet and triplet states using several methods. All optimized structures have then been proved by the harmonic vibrational frequency analysis whether to be stable minima on the global PES or not. Results indicate that for each spin state there exist three linear isomers and one cyclic isomer, but no bent conformer is found. All of these geometrical parameters and the harmonic frequencies are given in Table 1. The corresponding spin-density distribution, charge populations, and the zero-point vibrational energies for all of these stable species are collected in Table 2. Tables 3 and 4 list the calculated total energies (E_T) and the dissociation energies (D_e) of SiCO ground state $^3\Sigma^-$ dissociating into Si (^{3}P) and CO ($^1\Sigma^+$) and the corresponding state-state energy separations (ΔE) relative to the ground state, respectively. To test the bonding situation of the ground-state species, the vertical IP is also determined by comparing the energy difference between the ground-state species and their corresponding monovalent cation at the same geometrical configuration, and the results are also given in Table 3. The relevant transition state parameters are given in Table 5 for several state−state isomerization mechanisms. All triplet states are more stable than the corresponding singlet states. The linear SiCO in the triplet state with $^3\Sigma^-$ symmetry is the most stable and thus may be assigned to the global minimum. In addition, calculations have indicated that the spin contaminant

TABLE 1: Optimized Geometrical Parameters (Angstrom and Degree) and the Harmonic Vibrational Frequencies (cm^{-1}) at Different Theoretical Levels with a 6-311+G* Basis Set for SiCO Isomers

states	methods	r_{Si-C}	r_{Si-O}	r_{C-O}	$\angle_{ABC}$[a]	ω_1	ω_2	ω_3
SiCO	CASSCF	1.835		1.152	180.0	2178.1	360.2	548.7
($^3\Sigma^-$)	B3LYP	1.817		1.160	180.0	1955.2	321.5	573.7
(linear)	B3P86	1.810		1.157	180.0	1985.9	326.3	588.0
	B3PW91	1.814		1.158	180.0	1984.2	326.2	584.4
	MP2	1.825		1.161	180.0	1996.6	337.9	573.4
	CISD[31] [b]	1.835		1.157	180.0	2058	342	541
	CCSD(T)[33] [c]	1.825		1.159	180.0	1927	350	564
	Expt.[28]					1899.3		
SiCO	CASSCF	1.829		1.132	180.0	2155.8	338.7	578.2
($^1\Delta$)	B3LYP[d]	1.824		1.162	179.6	1958.5	265.5	576.0
(linear)	B3P86[d]	1.815		1.161	179.6	1983.6	264.7	591.9
	B3PW91[d]	1.818		1.161	179.5	1980.9	265.0	589.7
	MP2[d]	1.814		1.176	179.4	1907.0	266.1	610.5
SiCO	CASSCF	2.132	2.483	1.189	28.6			
(^{3}A″)	B3LYP	2.124	2.467	1.172	28.3	1780.6	107.6	277.3
(cyclic)	B3P86	2.029	2.344	1.182	30.3	1747.4	195.7	359.4
	B3PW91	2.051	2.369	1.179	29.9	1759.1	177.0	342.0
	MP2	2.118	2.461	1.172	28.4			
SiCO	CASSCF	2.000	1.768	1.251	38.1	1502.0	524.9	654.3
(^{1}A′)	B3LYP	1.964	1.809	1.280	39.4	1343.3	505.5	667.5
(cyclic)	B3P86	1.951	1.796	1.279	39.7	1359.0	534.8	690.1
	B3PW91	1.954	1.799	1.280	39.6	1354.9	529.5	688.5
	MP2	1.948	1.809	1.289	39.9	1338.6	531.0	673.3
SiOC	CASSCF		3.214	1.111	180.0	2388.6	47.5	55.3
($^3\Sigma^-$)	B3LYP		2.836	1.130	180.0	2184.0	66.0	66.8
(linear)	B3P86		2.617	1.131	180.0	2174.9	81.0	82.5
	B3PW91		2.765	1.130	180.0	2189.4	67.0	70.8
	MP2		3.019	1.140	180.0	2124.8	20.2	75.1
SiOC	CASSCF		3.196	1.110	180.0	2224.6	72.7	50.6
($^1\Delta$)	B3LYP[d]		2.392	1.139	179.6	2045.8	78.6	165.6
(linear)	B3P86[d]		1.923	1.169	179.8	1752.3	197.5	301.2
	B3PW91[d]		1.961	1.166	179.7	1779.6	174.3	291.0
	MP2[d]		2.924	1.140	179.8	2120.2	58.6	40.7
CSiO	CASSCF	1.857	1.483		180.0	1408.2	52.1	641.4
($^3\Sigma^-$)	B3LYP	1.846	1.524		180.0	1244.3	59.3	656.1
(linear)	B3P86	1.837	1.519		180.0	1263.4	71.4	682.1
	B3PW91	1.841	1.521		180.0	1258.9	62.7	677.8
	MP2	1.845	1.531		180.0	1247.8	48.0	695.0
	CCSD(T)[30][e]	1.852	1.521		180.0	1247.0	60.0	667.0
CSiO	CASSCF	1.854	1.486		180.0	1400.2	88.6	676.3
($^1\Delta$)	B3LYP[d]	1.836	1.529		179.8	1228.5	120.0	703.3
(linear)	B3P86[d]	1.829	1.524		179.7	1242.9	124.3	721.8
	B3PW91[d]	1.831	1.526		179.7	1239.0	122.9	719.0
	MP2[d]	1.839	1.538		179.5	1228.6	97.5	746.2

[a] ∠ABC for linear SiCO is referred to ∠SiCO, that for cyclic species is referred to ∠OSiC, that for linear SiOC species is referred to ∠SiOC, and that for linear OSiC species is referred to ∠OsiC. [b] Using DZ+P basis set and the frozen-core approximation. [c] Using TZ+3P(2f) basis set and the frozen-core approximation. [d] Estimated by reducing $^1\Delta$ symmetry to ^{1}A′ symmetry of the bent species. [e] Using cc-pVQZ basis set and the frozen-core approxiamtion.

TABLE 2: Calculated Spin-density Distribution (ρ), the Charge Population (Q), and the Zero-Point Vibrational Energies (ZPVE, in kcal/mol) for SiCO Isomers at Different Levels of Theory with the 6-311+G* Basis Set

states	methods	Q_{Si}	Q_C	Q_O	ρ_{Si}	ρ_C	ρ_O	ZPVE
SiCO	CASSCF	0.140	0.057	−0.197				
($^3\Sigma^-$)	B3LYP	0.180	−0.069	−0.111	1.311	0.361	0.329	4.53
(linear)	B3P86	0.144	−0.044	−0.100	1.319	0.352	0.329	4.61
	B3PW91	0.117	−0.014	−0.103	1.329	0.344	0.327	4.62
	MP2(full)	0.158	0.019	−0.177	1.496	0.103	0.402	4.64
SiCO	CASSCF	0.186	0.022	−0.208				
($^1\Delta$)	B3LYP	0.194	−0.084	−0.110				4.54
(linear)	B3P86	0.155	−0.054	−0.101				4.60
	B3PW91	0.134	−0.031	−0.103				4.59
	MP2(full)	0.216	−0.012	−0.205				4.49
SiCO	CASSCF	0.182	−0.144	−0.038				
(^{3}A″)	B3LYP	0.188	−0.156	−0.032	1.499	0.371	0.131	3.10
(cyclic)	B3P86	0.193	−0.169	−0.024	1.395	0.444	0.161	3.29
	B3PW91	0.173	−0.166	−0.007	1.434	0.422	0.144	3.26
SiCO	CASSCF	0.337	−0.280	−0.057				
(^{1}A′)	B3LYP	0.368	−0.351	−0.018				3.60
(cyclic)	B3P86	0.323	−0.343	0.020				3.69
	B3PW91	0.305	−0.343	0.038				3.68
	MP2(full)	0.449	−0.303	−0.145				3.64
SiOC	CASSCF	−0.020	0.017	−0.050				
($^3\Sigma^-$)	B3LYP	0.005	−0.024	0.019	2.023	0.010	−0.033	3.41
(linear)	B3P86	0.004	−0.089	0.085	2.020	−0.045	0.025	3.46
	B3PW91	0.003	−0.092	0.089	2.039	−0.042	0.012	3.20
	MP2(full)	−0.020	0.073	−0.053	2.066	−0.057	−0.008	3.42
SiOC	CASSCF	−0.021	0.057	−0.037				
($^1\Delta$)	B3LYP	0.042	−0.061	0.020				3.39
(linear)	B3P86	0.082	−0.206	0.124				3.50
	B3PW91	0.073	−0.215	0.142				3.46
	MP2(full)	−0.029	0.074	−0.045				3.20
CSiO	CASSCF	0.911	0.385	−0.526				
($^3\Sigma^-$)	B3LYP	0.766	−0.361	−0.406	0.272	1.586	0.142	2.81
(linear)	B3P86	0.746	−0.361	−0.385	0.294	1.573	0.134	2.89
	B3PW91	0.736	−0.366	−0.370	0.286	1.580	0.134	2.86
	MP2(full)	0.965	−0.420	−0.545	0.163	1.730	0.107	2.84
CSiO	CASSCF	0.874	−0.342	−0.532				
($^1\Delta$)	B3LYP	0.738	−0.335	−0.403				2.29
(linear)	B3P86	0.712	−0.332	−0.380				2.98
	B3PW91	0.700	−0.334	−0.366				2.96
	MP2(full)	0.934	−0.386	−0.548				2.95

TABLE 3: Calculated Total Energies (E_T, a.u.), the Dissociation Energies (D_e, kcal/mol), and the Vertical Ionization Potentials (IP_v, in kcal/mol) of SiCO in the Ground State at 6-311+G* Basis Set Level

	E_T ($^3\Sigma^-$) (linear)	D_e ($^3\Sigma^-$) (linear)	IP_v ($^3\Sigma^-$) (linear)
B3LYP	−402.8014836	36.50	202.12
B3P86	−403.2931744	41.50	217.32
B3PW91	−402.6998963	39.56	205.05
MP2	−402.1787529	28.89	190.01
MP4	−402.1926862	23.71	189.73
CCSD(T)	−402.2104139	26.17	189.83
CASSCF-MP2	−402.1799287	42.52	188.78

Note: For D_e, the dissociation mode is SiCO($^3\Sigma^-$) → Si (^{3}P) + CO ($^1\Sigma^+$).

is relatively small for the DFT and MP2 methods used in this work, and the averaged value of $\langle S^2 \rangle$ after annihilation of the first spin contaminant is very close to standard one. Therefore, it can be claimed that the results obtained here using the DFT, MP2, and other methods are reliable.

In the following sections, the discussions are divided into four parts according to their different structural characterization.

3.1. Linear SiCO Species. For this linear structure, there is one stable minimum on each corresponding global PES of each spin state. The triplet state ($^3\Sigma^-$) is significantly more stable than the singlet state ($^1\Delta$); the calculated ΔE is 17.26 kcal/mol at CASSCF-MP2 level. By using approximately estimated singlet state ($^1\Delta$) energy, the calculated ΔE is within 16−21 kcal/mol at several other theoretical levels. The results (18.2∼20.8 kcal/mol) at three DFT methods are in good agreement with each other and with the MP2 value (19.8 kcal/mol). They are slightly greater than the CASSCF-MP2 result. However, the estimates from MP4 and CCSD(T) are very close to the CASSCF-MP2 one. This relative regularity for the results at these DFT and CCSD(T) levels is very similar to that found for the other particular systems.[34−39] Thus, it can be concluded that ΔE being about 17 kcal/mol should be reliable.

Although these two states have a significant energy difference, they possess similar structures. For the ground state ($^3\Sigma^-$), at the CASSCF level, the optimized Si−C bond length is 1.835 Å, and it is very close to the CISD/DZ+P (1.835 Å)[31] and CCSD(T)/cc-pVQZ (1.825 Å)[33] results. The MP2 gives 1.825 Å, whereas three DFT levels yield the Si−C bond length within

TABLE 4: Calculated State−State Energy Separations (ΔE, in kcal/mol) Relative to the Ground States at 6-311+G* Basis Set Level[a]

	$\Delta E(^1\Delta)$ SiCO (linear)	$\Delta E(^3A'')$ SiCO (cyclic)	$\Delta E(^1A')$ SiCO (cyclic)	$\Delta E(^3\Sigma^-)$ SiOC (linear)	$\Delta E(^1\Delta)$ SiOC (linear)	$\Delta E(^3\Sigma^-)$ CSiO (linear)	$\Delta E(^1\Delta)$ CSiO (linear)
B3LYP	18.21	37.47	38.51	35.33	60.30	75.18	102.04
B3P86	20.23	38.69	39.33	39.96	65.37	77.13	106.12
B3PW91	20.80	38.64	40.43	38.75	66.02	77.18	107.06
MP2	19.84	39.11	39.89	26.91	59.72	75.66	104.85
MP4	17.26	35.31	36.07	21.80	51.92	73.92	100.62
CCSD(T)	16.36	32.97	34.32	24.04	49.88	73.35	97.63
CASSCF-MP2	17.26	43.24	45.39	45.24	55.46	75.58	94.03

[a] For the $^1\Delta$ state, the used total energies are estimated from the quasi-linear $^1A'$ state for DFT, MPn, and CCSD(T) methods.

TABLE 5: Optimized Parameters of Several Transition States at the B3LYP/6-311+G* Level

	$TS_{31}(^3A'')$	$TS_{32}(^3A'')$	$TS_{33}(^3A'')$	$TS_{11}(^1A')$	$TS_{12}(^1A')$	$TS_{13}(^1A')$
Si−C/Å	2.2956	3.3035	1.9345	2.4140	3.7537	1.9218
Si−O/Å	2.6411	3.0349	1.5621	2.4253	3.0766	1.5994
C−O/Å	1.1536	1.1302	2.5990	1.1565	1.1306	2.5853
∠SiCO/°	94.06	66.54	36.75	76.72	45.93	38.10
ω_1/cm^{-1}	75.95 **i**	67.00 **i**	625.21 **i**	176.95 **i**	93.22 **i**	652.75 **i**
ω_2/cm^{-1}	211.31	64.20	504.71	267.41	65.35	589.66
ω_3/cm^{-1}	1887.00	2186.39	1082.25	1923.74	2181.73	968.27
ΔE(TS)/kcal/mol[a]	37.55	40.21	95.67	54.00	61.81	131.29
E_{TS}/kcal/mol[a]	37.55	2.74	58.02	35.79	23.30	92.78
	0.08	4.88	20.49	15.49	1.51	29.25
ΔE(TS)/kcal/mol[b]	46.02	46.28	97.88	61.17	63.45	138.44
E_{TS}/kcal/mol[b]	46.02	3.04	54.64	43.91	18.06	93.05
	2.78	1.04	22.30	15.78	7.99	44.41

[a] ΔE(TS) denotes the energy separations of the transition state related to the ground state (the linear SiCO ($^3\Sigma^-$) species), whereas E_{TS} is referred to the activation barriers for the isomerization. The data in the first line for E_{TS} are those for the forward isomerization (from the left to the right in Figure 2), whereas the data in the second line are those for the backward isomerization (from the right to the left in Figure 2). [b] The same as in footnote a for the data format, but they are calculated by the CASSCF-MP2(full)/6-311+G* method at B3LYP/6-311+G* geometries.

1.810−1.817 Å. They are shorter than the CASSCF value by ca. 0.015 Å. For the C−O bond length, several methods give very close values to each other, and they are within 1.157−1.161 Å with ca. 0.004 Å of a largest deviation. Since the experimental detection of the linear SiCO ($^3\Sigma^-$) by Weltner and co-workers, there have been several theoretical investigations which focus on its structural property problem. Cai et al. optimized the Si−C bond length of SiCO ($^3\Sigma^-$) to be 1.835 Å and the C−O bond to be 1.167 Å at the multireference single and double excitation configuration interaction (MRSDCI) level with a double-ζ plus polarization basis set.[47] Using the same basis set (DZ+P), Dekock co-workers gave Si−C and C−O bond lengths to be 1.886 and 1.145 Å at the CASSCF level, whereas at the CISD/TZ+2P level, they obtained these two bond lengths as 1.839 and 1.139 Å.[31] Obviously, our CASSCF/6-311+G* bond lengths (1.835 and 1.152 Å) agree well with these same level results. In a recently detailed study on this species, Petraco co-workers used the higher-level (CCSD(T)) method and a larger basis set (TZ+3P(2f)) to give the Si−C and C−O bond lengths of 1.825 and 1.159 Å, respectively. No experimental values for these two bonds in the linear SiCO ($^3\Sigma^-$) molecule have been reported so far. Therefore, the highest-level theoretical value may be taken as the reference standard. Obviously, at the double-ζ level, even if the higher-level correlation correction methods (MRSDCI, CASSCF, CISD, etc.) are used, the bond length of Si−C is overestimated by 0.01−0.06 Å, whereas the C−O bond length is underestimated. At the triple-ζ level, the electronic correlation effects significantly shorten the Si−C bond by 0.02−0.04 Å and elongate the C−O bond. Comparison of our CASSCF, DFT, and MP2 results at the 6-311+G* basis set level with the Schaefer's CCSD(T)/TZ+3P(2f) value has fully indicated a good agreement among them. This phenomenon has implied that the theoretical methods (CASSCF, DFT, and MP2) used in this work are completely reliable for the treatment of these triplet state systems and can give the results very close to those from the highest-level correlation correction and multireference configuration methods.

For SiCO species in the singlet state ($^1\Delta$), because it exhibits multireference character, all methods which are based on the single determinant wave function are not suitable to treat its $^1\Delta$ state, and the CASSCF method becomes advantageous one. No any experimental works have been reported so far for this state. Only Cai et al. gave the bond length values (1.828 and 1.170 Å).[47] Our optimized bond lengths are 1.829 Å for the Si−C bond and 1.132 Å for the C−O bond, respectively. By starting from bent geometry, our DFT and MP2 optimizations give a quasi-linear configuration with the $^1A'$ symmetry; the ∠SiCO bond angle is about 179.5°, whereas the Si−C and C−O bond lengths are 1.814−1.824 and 1.161−1.176 Å, respectively. The vibrational frequency analysis also gives the evidence that this quasilinear configuration is really a minimum on the potential energy surface (no imaginary frequencies exist). Taking as a reference, these DFT and MP2 results are also given in Table 1. Although the Si−C bond length values at the DFT and MP2 levels are slightly shorter than that at the CASSCF level, they also implies a tendency that the Si−C bond length in the $^1\Delta$ state should be within 1.814−1.829 Å. The C−O bond in the $^1\Delta$ state is slightly longer than that in the $^3\Sigma^-$ state. Compared with the C−O bond length values (1.127−1.139 Å calculated at DFT and MP2 levels) of the free state CO ($^1\Sigma^+$), the C−O bond becomes longer by ca. 0.036 Å after combining with a Si atom and is very close to that (1.182−1.189 Å) of the free state CO^- ($^2\Pi$) anion. This phenomenon has indicated that the combination of Si with CO ($^1\Sigma^+$) has weakened the C−O bonding strength and caused the $CO^{\delta-}$ moiety in SiCO to possess the CO^- anion character. From the optimized Si−C

bond length, it also may be known that the Si−C bonds in SiCO ($^3\Sigma^-$ and $^1\Delta$) species are slightly shorter than the common Si−C single bond by ca. 0.05 Å, compared to 1.865 Å which occurred in ref 29, and are significantly longer than the common triple bond (1.588 Å[48]) by ca. 0.23 Å. This observation has implied that from the viewpoint of the bond length the Si−C bonds of the linear SiCO species in both states may be considered as the weak double-bond consisting of perhaps a σ bonding and a weak π bonding or the weak σ and π bonding. The following vibrational frequency analysis and the charge-transfer case can further demonstrate this prediction.

For the ground-state SiCO ($^3\Sigma^-$), there are one bending vibrational mode (ω_2 in Table 1) and two stretching−compression modes (ω_1 and ω_3 in Table 1). The bending mode is referred to the distortion of the linear molecule into bent one. The calculated bending vibrational frequency is in the range from 322 to 338 cm^{-1} at DFT and MP2 levels. At the CASSCF level, this frequency, being 360 cm^{-1}, is greater than DFT and MP2 values only by 23−38 cm^{-1}. These slightly small bending vibrational frequencies imply that the PES for the bending is flat. No experimental values have been reported for this vibrational mode. However, an early experimental report had implied this low-bending vibrational mode.[28] From the ESR data,[28] it appears that the SiCO molecule also may be bent in some sites in some matrixes, and at least SiCO in argon is the case where almost all molecules appear to be nonlinear. However, our calculations on SiCO species have confirmed that a small departure from the linearity can be expected to be slightly unstable with respect to the linear conformation. However, the energy increase is very small (only ca. 0.6 kcal/mol at B3LYP/6-311+G* level) when the ∠SiCO bond angle changes from 180° to 170° or other smaller ones. This is to say that the bending force constant is quite small and some constraints in the matrix sites may induce bending. This easy bending tendency may be also attributed to the existence of the weak interaction between Si and CO moieties. In fact, there are two weak π-bonding interactions between Si and CO moieties besides the weak σ bond.

Another two vibrational modes may be assigned to the Si−C and C−O stretching vibrations, respectively. At DFT and MP2 levels, the calculated harmonic frequencies are within 573−584 and 1955−1996 cm^{-1}, whereas at CASSCF level, the values are 2178 and 548 cm^{-1} for the ground state ($^3\Sigma^-$), respectively. For the $^1\Delta$ state, the CASSCF yields 2155 and 578 cm^{-1} for two stretching modes, respectively. As mentioned above, DFT and MP2 methods are not suitable to treat this linear $^1\Delta$ state; thus, the frequencies in the $^1\Delta$ state are also estimated by reducing its symmetry to $^1A'$ to be within 577−610 and 1906−1984 cm^{-1} at the DFT and MP2 levels. Although these frequencies cannot correspond to the accurate ones, they also imply the frequency range. Very good agreement can be observed for every vibrational modes of every species for several theoretical methods. Only the C−O mode of SiCO in the ground state ($^3\Sigma^-$) has been experimentally observed to be 1899.3 cm^{-1},[28] and no report on other vibrational modes has been given. The experimental estimate for the later is ca. 800 cm^{-1}. For the $^3\Sigma^-$ state, at the CISD/DZ+P level, Schaefer and co-workers calculated the Si−C and C−O stretching frequencies to be 541 and 2058 cm^{-1}, respectively,[31] whereas in another detailed investigation, they gave many calculated results, falling with 471−564 cm^{-1} for Si−C stretching and 1927−2214 cm^{-1} for C−O stretching at SCF, CCSD, and CISD levels of theory with a series of triple-ζ basis sets. Cai et al. also determined the Si−C and C−O stretching frequencies to be 873 and 2105 cm^{-1}, respectively, at the MRSDCI/DZ+P level.[47] Among these studies regarding SiCO ground state ($^3\Sigma^-$), the used highest-level method should be the CCSD(T)/TZ+3P(2f) method; it yields 564 cm^{-1} for the Si−C stretching and 1927 cm^{-1} for the C−O stretching, respectively. All of these results have exhibited such a tendency that correlation effects can significantly decrease the vibrational frequency of the C−O stretching (by ca. 200−300 cm^{-1}) and, at the same time, increase that of the Si−C stretching. Thus, it is very important to consider the electronic correlation in the relevant calculations. It is well-known that DFT is another method which takes the electronic correlation correction into account and has been proved to be a reliable and computationally inexpensive method that is capable of successfully predicting the properties for many systems. Our calculated value for Si−C stretching of SiCO ($^3\Sigma^-$) at three DFT and MP2 levels is slightly larger than the corresponding CCSD(T)/TZ+3P(2f) value by 9∼23 cm^{-1}. They are significantly smaller than the experimental estimate (800 cm^{-1}) by 213−227 cm^{-1}. Overall analysis has indicated that Lembke et al. overestimated the Si−C stretching frequency by about 40%. Cai et al.'s result (873 cm^{-1}) from the DZP MRSDCI method also appears to be too large.[47] For the C−O stretching in $^3\Sigma^-$ state, our calculated values are slightly greater than the experimental value (1899.3 cm^{-1}) by 56−96 cm^{-1} and are very close to the CCSD(T)/TZ+3P(2f) value (1927 cm^{-1}). Obviously, the deviation between the theoretical and the experimental values for the C−O mode of SiCO ($^3\Sigma^-$) is almost equivalent to that (within 80 cm^{-1}) which occurred in the free state CO ($^1\Sigma^+$). Unfortunately, as with other electron correlation methods (CCSD, etc.), the CASSCF method seemly also overestimates this frequency value by 100−200 cm^{-1}. Comparison between free CO and bounded CO reveals that the absolute change in the C−O vibrational mode is significant after combination of CO with Si. The frequency red-shift is 85 cm^{-1} at the CASSCF/6-311+G* level, 238−258 cm^{-1} at the DFT/6-311+G* level, and 133 cm^{-1} at the MP2/6-311+G* level. They, especially the DFT results, are very close to the experimental red-shift value (245 cm^{-1}). The considerable decrease in the C−O mode frequency implies the weakening of the C−O bonding, and this weakening is greater than that in the transition metal MCO systems. From above analysis, it seemly implies that the Si−C bonding of SiCO species in the ground state is weak. Similar analysis may be true for the $^1\Delta$ state, and the accuracy of the relevant results should be also reliable.

However, D_e behaves as another tendency. No theoretical and experimental estimates for D_e have been reported for the linear SiCO $^3\Sigma^-$ species. Table 4 lists D_e calculated values of SiCO ($^3\Sigma^-$) dissociating into Si (^{3}P) and CO ($^1\Sigma^+$) using several different methods. No zero-point energy and counterpoise corrections have been made for these D_e values. The corrections may slightly reduce the values but do not significantly change the relative regularity. Thus, the discussion will emphasize the qualitative analysis. Three DFT methods give the results within 36.5−41.5 kcal/mol, being considerably greater than the MP2 values by 8−13 kcal/mol. The high-level CCSD(T) method at MP2 geometry yields D_e to be 26.1 kcal/mol, whereas MP4 underestimates this value by 2.5 kcal/mol. On the basis of the CASSCF/6-311+G* geometry, D_e is also calculated with the CASSCF-MP2/6-311+G* method, being 42.5 kcal/mol. This value is close to three DFT results but is significantly larger that all other values at the wave function-correlated levels. The CASSCF-MP2/6-311+G*//CASSCF/6-311+G* method overestimates the D_e value. Obviously, the deviations in the D_e estimates should be attributed to such a fact that the CASSCF/

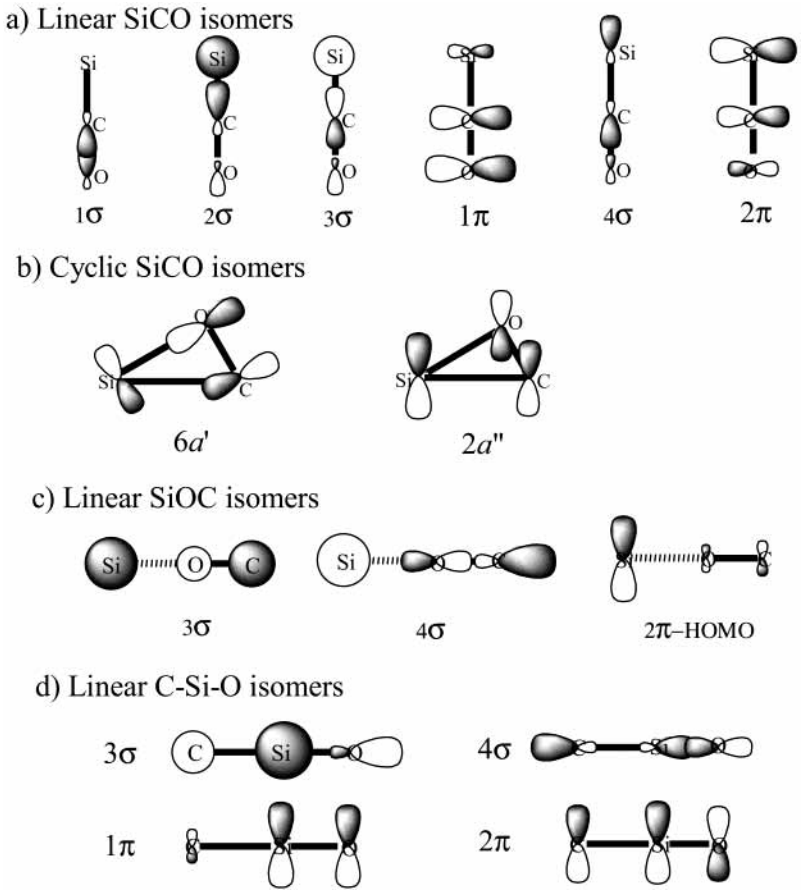

Figure 1. Orbital interaction diagram for several isomers.

6-311+G* geometries were used instead of the CASSCF-MP2/6-311+G* geometries, because the later method requires much computational cost. Although the proper configurations are included in the CASSCF method, no electron correlation correction is taken into account. It may be predicted that the D_e can be correctly estimated to be smaller than the present value by using the CASSCF-MP2 method at the CASSCF-MP2 geometries. Although there is a significant difference between DFT values and those from the correlated-wave function methods, D_e being at least 26 kcal/mol is reliable. These D_e values have implied that the Si−CO bonding should not be considered as a very weak interaction. It is weaker than the common chemical bonding and stronger than the intermolecular weak interaction. This prediction is basically in agreement with the above analysis.

Another important quantity is the ionization potential. No experimental and theoretical estimates have also been reported so far for SiCO IP. Table 4 only lists our calculated values for the vertical IP of the SiCO $^3\Sigma^-$ state. Several theoretical methods give good consistent results, and the relative error is only 7% of the total IP_V. In particular, the CASSCF-MP2 value is almost equal to the CCSD(T) one. Therefore, it can be concluded that the values being 190−200 kcal/mol are reliable for the SiCO $^3\Sigma^-$ state species. IP_v denotes the energy required for removing an electron from the frontier orbital under Franck−Condon condition. These large IP_v values indicate that the frontier orbital energy level is very low and the electrons occupied on it are very stable. These IP_v values are greater only by ∼16 kcal/mol than the Si atomic IP results (186.74, 201.24, 190.45, and 179.19 kcal/mol for three DFT and CCSD(T) methods), indicating that Si moiety in SiCO ($^3\Sigma^-$) still keeps the Si atomic character. The ionized electron mainly comes from Si center.

All these special phenomena observed here strongly depend on the interesting bonding character. The valence electronic configurations for $^3\Sigma^-$ and $^1\Delta$ states are, respectively

$$^3\Sigma^-: \text{ [core]}(1\sigma^2)(2\sigma^2)(3\sigma^2)(1\pi^4)(4\sigma^2)(2\pi_+^1)(2\pi_-^1)(5\sigma^0)$$

$$^1\Delta: \text{ [core]}(1\sigma^2)(2\sigma^2)(3\sigma^2)(1\pi^4)(4\sigma^2)(2\pi_+^2)(2\pi_-^0)(5\sigma^0)$$

$$\text{or [core]}(1\sigma^2)(2\sigma^2)(3\sigma^2)(1\pi^4)(4\sigma^2)(2\pi_-^2)(2\pi_+^0)(5\sigma^0)$$

All of the bonding molecular orbitals have been drawn in Figure 1 (see Figure 1a). The major difference between the two electronic states originates from the different occupation of the highest-occupied molecular orbital (HOMO) and a couple of degenerate π orbitals. Obviously, this $^1\Delta$ state should be energetically higher than the $^3\Sigma^-$ state. For the $^3\Sigma^-$ state, there is only one occupation scheme $(2\pi_+^1)(2\pi_-^1)$. However, for the $^1\Delta$ state, there are two occupation ways: $(2\pi_+^2)(2\pi_-^0)$ $(2\pi_+^0)(2\pi_-^2)$. Therefore, the $^3\Sigma^-$ state is referred to as the single-determinant state, whereas the $^1\Delta$ state should be referred to as at least the two-Slater-determinant state. Inspection of the frontier orbitals reveals that these degenerate π orbitals (HOMO) consists of Si p-orbitals and CO antibonding π^* orbitals. These orbitals describe the bonding interaction between Si and C centers and the antibonding interaction between C and O centers (see Figure 1a, 2π MO). Thus, it can be predicted that, in the formation process, Si being an acceptor uses its empty p orbital to accept the coordination lone pair electrons of the donor CO, yielding the high-energy-level backbone σ-type bonding ($4\sigma^2$), at the same time, the formation of the π bonds further strengthens the Si−C bonding interaction and weakens the C−O interaction because of the feedback of Si π-type electrons to

the π^* orbitals of CO. This bonding mechanism seemly is similar to that which occurred in the transition metal carbonyls, but a major difference of SiCO from MCO is that Si uses its p-type orbitals to form the feedback π bond instead of the d-type orbitals. The weakening of C−O bonding in the SiCO species is greater than that in the transition metal carbonyl complexes, MCO. The analysis about the charge population also reveals that the net charge transfers from Si to CO are 0.12−0.18 e for SiCO ($^3\Sigma^-$), and the transferred charges mainly distribute over the O center. However, the spin density distribution reflects that SiCO ($^3\Sigma^-$) exhibits the character of silene (the carbene-like) and may be named as carbonylsilene. Of two spin single electrons 1.3−1.5 e distribute over the Si center, whereas the remains are equivalently over the C (∼0.35e) and O (∼0.33e) centers. This phenomenon has also implied that two degenerate HOMOs with two spin unpaired electrons mainly describe the Si π-type orbital character. This is consistent with IP_v analysis. Calculations on the ionized $SiCO^+$ species indicate that when an electron is removed the SiCO ($^3\Sigma^-$) state becomes the $SiCO^+$ ($^2\Pi$) state. In the later, the positive charge is mainly over the Si center with +0.7 to +0.8, and the left one spin unpaired electron is also distributed over the Si center with a considerable amount of ∼0.79. Compared with the distribution of SiCO ($^3\Sigma^-$), it can be confirmed that the ionized electron is the HOMO π electron with significant Si p_π-type orbital character. Similar analysis is also true for the SiCO $^1\Delta$ state. In addition, it should be noted that, although in the bond length aspect the $CO^{\delta-}$ moiety of SiCO exhibits the CO^- character, the spin density is considerably different from the CO^- species (C: ∼1.0 and O: ∼0.0), and there is also a large charge distribution difference between them. Thus, $CO^{\delta-}$ cannot be classified as CO^- anion species, such as these occurred in MCO (M = alkali metals).

3.2. Cyclic SiCO Species. There exist cyclic isomers for SiCO species in triplet and singlet states. The cyclic triplet state is referred to as $^3A''$, reduced from the linear SiCO $^3\Sigma^-$ state by bending, whereas the cyclic singlet state is referred to as the $^1A'$ state, reduced from the linear SiCO $^1\Delta$ state. These two cyclic isomers are energetically very close to each other; the energy separation is only ca. 1−2 kcal/mol. However, their geometric structures are significantly different. The $^3A''$ Si−C bond length is within 2.05−2.12 Å and is longer than that in the $^1A'$ state by 0.10−0.16 Å. They are considerably longer by ca. 0.21 and ca. 0.14 Å than those of the corresponding linear SiCO species ($^3\Sigma^-$, $^1\Delta$). Similarly, the Si−O bond (2.37−2.46 Å) of the $^3A''$ state is also significantly longer by 0.55−0.60 Å than that in the $^1A'$ state. Another difference between $^3A''$ and $^1A'$ states is that of the C−O bond. The $^3A''$ C−O bond falls within 1.17−1.18 Å and is shorter by ca. 0.1 Å than that (ca. 1.28 Å) of the $^1A'$ state. Obviously, the C−O bond in the $^3A''$ state is slightly longer than those of the linear SiCO structures and is also longer only by ca. 0.04 Å than the free state C−O bond (1.127−1.139 Å). These results have indicated that $^3A''$ combination between Si (^3P) and CO ($^1\Sigma^+$) has slightly weakened the C−O bond, but does not rupture it; it still keeps some C−O structural character. However, for the $^1A'$ state, the C−O bond is significantly longer than the free state CO bond. This phenomenon has implied that the C−O bond has been greatly weakened after combining with Si according to $^1A'$ state coupling mechanism.

For these two cyclic species, each has three vibrational modes. ω_2 corresponds to the symmetric stretching vibration between Si and CO, whereas ω_3 corresponds to the antisymmetric one. The more explicit assignment should be the ω_1 mode which corresponds to the C−O stretching vibration. The later two modes (ω_2, ω_3) especially for the ω_2 mode reflects the interaction strength between Si and CO. For the $^1A'$ state, DFT and MP2 predict ω_2 and ω_3 modes to be 505−534 and 667−690 cm^{-1}, whereas CASSCF gives 524.9 and 654.3 cm^{-1}, respectively. Obviously, both of these two modes are stronger than those in the $^3A''$ state. These frequency results have indicated that the bonding interaction between Si and CO moieties in each cyclic structure is considerably different from that of the linear SiCO in both states ($^3\Sigma^-$, $^1\Delta$). For the singlet state, the interaction between Si and CO in the cyclic isomer ($^1A'$) is stronger than that in the linear SiCO isomer ($^1\Delta$), but for the triplet state, the order is inverse (cyclic $^3A''$ < linear $^3\Sigma^-$). Obviously, this observation may be attributed to the different bonding mechanism among them. Another noticeable aspect is the C−O stretching vibration. The ω_1 for the $^1A'$ state is smaller by 390−440 cm^{-1} than that for the $^3A''$ state. They are significantly smaller than that (2129−2263 cm^{-1}) of the free state CO, but they are relatively close to that (1649−1796 cm^{-1}) of the free state CO^-. In particular, the CO moiety in cyclic $^3A''$ SiCO species is very similar to the free state CO^- not only in the C−O bond length but also in the vibrational frequency. This shows that the CO moiety in the cyclic SiCO isomer behaves as the free state CO^- anion character.

All of these observations may be interpreted well by their bonding mechanism. The valence electronic configurations for the cyclic isomers in both states are

$$^3A'': \ (1a')^2(2a')^2(3a')^2(1a'')^2(4a')^2(5a')^2(6a')^1(2a'')^1$$

$$^1A': \ (1a')^2(2a')^2(3a')^2(1a'')^2(4a')^2(5a')^2(6a')^2(2a'')^0$$

Two key orbitals $6a'$ and $2a''$ have been drawn in Figure 1b. Obviously, the main difference between these cyclic isomers with different spin states should be attributed to the different occupations of the frontier orbitals ($2a''$ and $6a'$). Comparison between these two electronic configurations reveals that the exchange occupation between $2a''$ and $6a'$ orbitals may yield two different electronic states ($^3A''$ and $^1A'$). By inspecting $2a''$ and $6a'$ orbitals, it can be known that the $2a''$ orbital is an out-of-plane π-type orbital principally describing the interaction between the Si $p_\perp$-type orbital and the π^*-antibonding orbital of CO moiety, whereas $6a'$ is an in-plane bonding orbital, principally describing the bonding interaction between Si $p_{||}$-type orbital and the in-plane π^*-antibonding orbital of CO moiety. For the cyclic $^1A'$ state, two electrons occupy the $6a'$ orbital (HOMO), and the $2a''$ is empty (LUMO). This occupation strengthens the bonding between Si and C centers and between Si and O centers and, at the same time, reduces the bonding between C and O centers, resulting in shorter Si−C and Si−O bonds and a slightly longer C−O bond. Obviously, when an electron is removed from $6a'$ orbital, the Si−C and Si−O bonds will be weakened, and the C−O bond will be strengthened. Similarly, when an electron is added to the $2a''$ orbital, the Si−C π-bonding interaction increases, and the π^*-antibonding interaction of the Si−O and C−O bonds increases. Therefore, the transfer of a $6a'$ electron to $2a''$ orbital, yielding the $^3A''$ state, may result qualitatively in the following three aspects of changes: (i) reducing Si−C σ bonding, increasing Si−C π-bonding, and the net change is that Si−C bond becomes slightly weak; (ii) reducing Si−O σ bonding ands increasing Si−O π^*-antibonding interaction, and the net change is that the Si−O bond is greatly weakened; (iii) reducing in-plane π^*-antibonding interaction and increasing out-of-plane π^*-antibonding interaction between C and O, and the net result is that the C−O bond is seemly unchanged. Actually, for case iii, if

the different electron density distribution over three centers (Si, C, and O) between the $2a''$ and $6a'$ orbitals is considered, the C−O bonding change caused by the excitation of $6a'$ electron to the $2a''$ orbital may be easily distinguished. Comparison of the molecular orbital combination coefficients of $2a''$ and $6a'$ orbitals reveals that the orbital component of the Si center in $2a''$ is greater than that in $6a'$, and the transfer of a $6a'$ electron to $2a''$ actually reduces the electron population in π*-antibonding orbital of C−O moiety; thus, the net contribution from the transfer ($6a' \rightarrow 2a''$) to the C−O bonding is the increase of bonding interaction. The reflection of these significant changes in the molecular geometric parameters is that the Si−C becomes slightly longer, the Si−O bond becomes much longer, but the C−O bond becomes slightly shorter than those in the singlet state. This analysis has been fully demonstrated by comparison of the geometric parameters in Table 1.

Actually, the bonding between Si and CO moieties may be attributed to the following mechanism. Si uses its in-plane *p* orbital to attack by side the in-plane π* antibonding orbital of CO, at the same time, Si also uses its out-of-plane *p* orbital to interact the out-of-plane π* of CO, forming the conjugated π bond. The formed two molecular orbitals should be occupied by two electrons donated by Si. Inspection of orbital components reveals that the charge-transfer amount from Si to CO should be that $^3A'' > {}^1A'$. The charge population in Table 2 has clearly shown the charge-transfer case. In addition, the spin-density distribution in Table 2 also demonstrates the charge transfer and bonding interaction. For the $^3A''$ state, the two unpaired spin electrons are mainly distributed over the Si center with a large amount of 70−75%, and only a small amount of these single-electrons are transferred into C (18−22%) and O (6−8%), indicating that the Si moiety in the cyclic $^3A''$ species still keeps the Si atomic character. The natural orbital analysis also reveals that there are two lone-electron orbitals which are localized at the Si center. So is the cyclic SiCO $^1A'$ state, but with the lone-pair electrons centered at Si.

Another interesting aspect for these cyclic species is that whether they may be classified as the epoxy compound or not. An important experimental phenomenon of the olefinic compounds in the oxidation processes is the production of the epoxy species, in which the π bond is substituted by the oxygen-bridging bond (−O−), forming a three-member cyclic structure. For example, the silicon-containing epoxy ethane (epoxy silaethane) may be produced from $H_2Si{=}CH_2$. The optimized Si−C, Si−O, and C−O bonds are 1.819, 1.686, and 1.485 Å, respectively, at the B3LYP/6-311+G* level, being obviously different from the corresponding those of the cyclic SiCO species. In particular, the C−O bond in the epoxy species is a typical C−O single bond (a σ-bonding) and is significantly different from that of carbon monoxide (CO), whereas that in cyclic SiCO species obviously keeps the character of carbon monoxide. Thus, it can be concluded that these cyclic SiCO in both states does not belong to the epoxy species, and should be the weak-interaction complex.

3.3. Linear SiOC Species. It is well-known that there is not an obvious charge population difference over the C and O centers in the CO molecule and its dipole moment is very small; thus, CO is not an electrostatics interactant. However, there are lone-pair electrons in both ends of the CO molecule; thus, CO may be also taken as a donor by the O end, interacting with the acceptors with the low-energy empty orbitals. Because the lone-pair electrons at the O end are energetically lower than that at the C end, it can be predicted that the donor ability by the O end is relatively smaller than that by the C end and that the formed complexes by the O end are generally less stable than the corresponding those by the C end. For the Si atom, there are five degenerate empty *d* orbitals. These empty *d* orbitals have provided a condition that Si may be taken as an acceptor. Therefore, it can be predicted that there should be a SiOC complex similar to the linear SiCO species. The geometric optimizations have fully confirmed this predication. The linear SiOC species in the triplet ($^3\Sigma^-$) and singlet ($^1\Delta$) states correspond, respectively, to minima on the triplet and singlet state PESs. For these two isomers, the $^3\Sigma^-$ state is lower by ca. 10 kcal/mol than $^1\Delta$ state at the CASSCF-MP2/6-311+G*//CASSCF/6-311+G* level, and they are significantly higher than the ground state by 24−45 and 50−60 kcal/mol, respectively, at several levels of theory. As occurred in the cyclic systems, comparison of CASSCF-MP2 results with those at other theoretical levels indicates that there is significant discrepancy between them. In particular, the CASSCF-MP2 results are generally larger than the CCSD(T), MP4, and MP2 ones. As mentioned above in discussion regarding the D_e of the ground-state SiCO ($^3\Sigma^-$) species, actually, this discrepancy should be attributed to the use of the CASSCF geometries instead of the CASSCF-MP2 geometries. Although the former method can produce the correct electronic configurations and yield accurate geometric parameters by taking into account the multiconfiguration determinants, it may yield larger deviation for the relevant energy quantities perhaps because it does not include the electron correlation correction. It may be predicted the direct optimization calculations at the CASSCF-MP2 level may give reasonable results for these energy quantities.

The optimized Si−O bond length in the $^3\Sigma^-$ state is 3.21 Å, whereas that in the $^1\Delta$ state is also about 3.2 Å at the CASSCF/6-311+G* level. DFT and MP2 methods yield an Si−O bond length of 2.6−3.2 Å for the $^3\Sigma^-$ state. For the the $^1\Delta$ state, the estimated Si−O bond length value from the quasi-linear SiOC $^1A'$ state is 1.9−2.9 Å. Obviously, the deviation for Si−O bond in the $^1\Delta$ state among DFT and MP2 results is up to 1.0 Å, indicating that these DFT and MP2 methods are not suitable to investigate this system in the $^1\Delta$ state. Comparison between the $^3\Sigma^-$ state and the $^1\Delta$ state reveals that the Si−O bond in the $^3\Sigma^-$ state is longer than that in the $^1\Delta$ state. At the CASSCF level, the calculated results are 3.214 Å (CASSCF/6-311+G*) and 3.268 Å (CASSCF/aug-cc-pvTZ) for the $^3\Sigma^-$ state, whereas that is 3.219 Å (CASSCF/6-311+G*) for the $^1\Delta$ state. Although there exist some deviations for the Si−O bond length at several theoretical levels, they are obviously longer than the general Si−O bond. However, for the C−O bond, the $^3\Sigma^-$ state is slightly shorter than the $^1\Delta$ state. Compared with those of the corresponding linear SiCO species, the C−O bond lengths in both states ($^3\Sigma^-$, $^1\Delta$) are slightly shorter than the corresponding ones of those of the linear SiCO species. This observation has fully indicated that the interaction of Si with the CO moiety by the O end belongs to the weak interaction for both states. This prediction may be proved by inspecting the harmonic frequencies.

For these two species, two important vibrational modes are ω_1 and ω_3 vibrations, and they are assigned to the SiO−C and Si−OC stretching vibrations. The other one (ω_2) is referred to the bending vibration. For the $^3\Sigma^-$ state, the calculated frequency for Si−OC (ω_3) vibration falls within 55−82 cm^{-1} and is far smaller than that for the common chemical bonding, whereas the corresponding C−O stretching frequency falls within 2124−2388 cm^{-1} and is very close to that of the free state CO molecule. The bending vibrational frequency is also within 20−81 cm^{-1}, denoting that the bending PES is flat and the

corresponding potential barrier is very low. Therefore, this molecule is structurally facile and is very easily distorted to the cyclic species. Similarly, for the $^1\Delta$ state, the CAASCF method predicts the frequencies to be 2224 (ω_1), 73 (ω_2), and 51 (ω_3), respectively. Because of the unsuitability of DFT and MP2 in treating $^1\Delta$ state of this system, the deviation among their theoretical results is large. By considering the bonding character of the $^3\Sigma^-$ state, it should be believed that the results obtained at the CASSCF/6-311+G* level are reliable, and perhaps the B3LYP and MP2 results (58−70 for ω_2, 40−110 for ω_3, and 2047−2122 cm^{-1} for ω_1) are fortunately reasonable. These small bending vibrational frequencies and small Si−OC stretching frequencies also imply that there should be similar PES character in the $^1\Delta$ state to that in the $^3\Sigma^-$ state.

The structural character mentioned above should be closely related to their bonding and the interaction nature. For these linear species (SiOC), the valence electronic configurations are

$$^3\Sigma^-:\ [\text{core}](1\sigma)^2(2\sigma)^2(1\pi_+)^2(1\pi_-)^2(3\sigma)^2(4\sigma)^2(2\pi_+)^1(2\pi_-)^1$$

$$^1\Delta:\ [\text{core}](1\sigma)^2(2\sigma)^2(1\pi_+)^2(1\pi_-)^2(3\sigma)^2(4\sigma)^2(2\pi_+)^2(2\pi_-)^0$$

Population analysis indicates that the important orbitals describing the interaction between Si and OC moieties are the 3σ and 4σ orbitals (see Figure 1c). 3σ reflects the s−s σ*-antibonding interaction between Si and O centers and that between O and C centers, whereas 4σ reflects the σ*-antibonding interaction between the s orbital of Si and the p-type σ bonding of the CO moiety. These two kinds of interactions are very weak. The HOMOs are degenerate π-type orbitals describing the interaction between the π-type p orbitals of Si and the π*-antibonding orbitals of CO. Actually, for each π orbital ($2\pi_+$ or $2\pi_-$), the component of the Si π-type p orbital is far greater than that of the CO π*-antibonding orbital, indicating that this orbital essentially denotes the π-type pure p orbital of the Si atom. Therefore, the open-shell occupation or the closed-shell occupation of HOMOs by two electrons does not significantly affect the chemical bonding of Si−OC. From analysis mentioned above, it can be known that the bonding interaction between Si and CO fragments by the O end is really very weak, and the molecules are structurally facile. The observed structural character should be that there is a longer Si−O bond with a smaller vibrational frequency, and that the $^3\Sigma^-$ state is structurally close to the $^1\Delta$ state. The very small dissociation energy (1.0∼2.0 kcal/mol) has also fully confirmed the above analysis.

Another interesting aspect lies in its bonding character different from the aether compounds. At the B3LYP/6-311+G* level, the substituted aether ($H_3Si-O-CH_3$) is optimized on the triplet and singlet states. There are two obvious differences between $H_3Si-O-CH_3$ aether and the linear SiOC species. First, there is a different state−state relative stability. The singlet state is more stable than the triplet state for the aether, whereas the triplet state ($^3\Sigma^-$) is more stable than the singlet state ($^1\Delta$) for the linear SiOC species. Second, there is a different optimized skeleton geometry consisting of Si, C, and O atoms. For the aether $H_3Si-O-CH_3$ species in singlet state (the ground state), the optimized ∠SiOC angle is 124.9°, whereas the optimized Si−O and O−C bond lengths are 1.66 and 1.42 Å, respectively. Therefore, it can be concluded that the linear SiOC in both states should not be classified as the aether compound.

In addition, the relative stability comparison of the linear SiOC species with the linear SiCO species in both states has also indicated that CO has two nucleophilic centers, viz., the O end and the C end, and the nucleophilic ability is that the C end is far greater than the O end. This observation agrees very well with the usual findings that CO is generally to use its C end to form the carbonyls.

3.4. Linear CSiO Species. Besides the isomers which have a direct C−O linkage, another isomer has also been detected which does not have the C−O linkage. The C and O atoms lie in the two sides of Si, and three atoms keep as a linear structure. This kind of isomer is energetically far higher than the linear SiCO isomers, and the corresponding energy-separations are 75kcal/mol and 94kcal/mol related to the ground state at the CASSCF/6-311+G* level. Also, the triplet state ($^3\Sigma^-$) is more stable than the singlet state ($^1\Delta$) by ca. 20 kcal/mol. Perhaps, this large ΔE should be attributed to the rupture of the C−O bond. In recent years, only one work focused on the theoretical calculation of this linear CSiO species in the $^3\Sigma^-$ and $^3\Pi$ states,[30] but no study on the singlet state has been reported. For the most stable triplet state ($^3\Sigma^-$) of this structure, Schaefer and coworkers optimized the C−Si and Si−O bond lengths to be 1.852 and 1.520 Å, respectively, at the CCSD(T)/cc-pVQZ level, the highest-level method used in their work. At the DFT/6-311+G* level, for this state, our optimized Si−C bond falls within 1.837−1.846 Å and the Si−O bond is within 1.519−1.531 Å. Obviously, these results are in good agreement with those at the CCSD(T)/cc-pVQZ level. These Si−C bonds are slightly longer than those of the most stable linear SiCO $^3\Sigma^-$ isomer by 0.02−0.03 Å. The Si−C bond length in the CSiO $^3\Sigma^-$ state is also longer than that of the $^3\Sigma^-$ free state SiC species (1.813 Å at the B3LYP/6-311+G* level), whereas that in the $^1\Delta$ state is close to that of the $^1\Sigma^+$ free state SiC species (1.837 Å at the B3LYP/6-311+G* level). The Si−O bonds in both states are also considerably shorter than those of the cyclic SiCO and the linear SiOC isomers, but they are very close to the Si−O bond (1.523 Å at the B3LYP/6-311+G* level) of the free state SiO species. From the structural viewpoint, the linear CSiO isomers in both states seem to be the analogue of the linear SiCO species. Namely, the linear CSiO may be seemingly taken as the combination of SiO (the analogue of CO) with C (the same group element as Si). It can be thought that these linear CSiO species are less stable than the corresponding SiCO species because of the ability of accepting electrons of C different from Si. Comparison of the data in Table 2 indicates that the charge transfers from the SiO moiety to C are 0.33−0.38 e for the $^1\Delta$ state and 0.36−0.42 e for the $^3\Sigma^-$ state, whereas for the linear SiCO species, the charge transfers are inversely from Si to the CO moiety. This phenomenon has reflected two facts: (i) SiO is a stronger donor and a weaker acceptor than CO and (ii) C is a better electron acceptor than Si.

The calculated valence electronic configurations are

$$^3\Sigma^-:\ [\text{core}](1\sigma)^2(2\sigma)^2(3\sigma)^2(1\pi_+)^2(1\pi_-)^2(4\sigma)^2(2\pi_+)^1(2\pi_-)^1$$

$$^1\Delta:\ [\text{core}](1\sigma)^2(2\sigma)^2(3\sigma)^2(1\pi_+)^2(1\pi_-)^2(4\sigma)^2(2\pi_+)^2(2\pi_-)^0$$

The bonding properties of some main orbitals have been described in Figure 1 (see Figure 1d). The 1σ and 2σ are referred to the σ-type s−s orbital interaction between Si and O and that between Si and C, respectively. 3σ reflects the σ bonding interaction between the Si s orbital and the O ($s + p_z$) orbitals and also synchronously reflects the antibonding interaction between the Si s orbital and the C s orbital. Another interesting σ bonding is 4σ, which describes the σ bonding interaction among the p_z orbitals (along the molecular axis) of Si, C, and O centers. In addition, the formation of two kinds of π bonds also significantly modifies the Si−C and Si−O bonding interaction. Obviously, the 1π molecular orbital is degenerate (π_+, π_-), and mainly describes the bonding interaction between

Si and O and the very weak antibonding interaction between Si and C, whereas the 2π orbital is degenerate (π_+, π_-) frontier orbitals, mainly describing the bonding interaction between Si and C and the antibonding interaction between Si and O. Because the HOMO is degenerate, two frontier orbital electrons are in preference to respectively occupy two degenerate π orbitals with the same spin-direction. Thus, the $^3\Sigma^-$ state should be more stable than the $^1\Delta$ state. This prediction has been proven by the data in Table 4. The main difference between the $^3\Sigma^-$ state and the $^1\Delta$ state lies in the different occupation of the HOMO. The state excitation from ($2\pi_+{}^1 2\pi_-{}^1$) to ($2\pi_+{}^2 2\pi_-{}^0$) significantly increases the electron repulsion energy but does not significantly change the bonding character among three atoms. This implies that the $^3\Sigma^-$ state and the $^1\Delta$ state are geometrically similar (compare Si−O 1.524 Å ($^3\Sigma^-$) with 1.529 Å ($^1\Delta$), and Si−C 1.846 Å ($^3\Sigma^-$) with 1.836 Å ($^1\Delta$) at the B3LYP/6-311+G* level). For the σ bonding interaction, the Si−O bonding strength is stronger than that of the Si−C bond. For the π bonding, the occupation of four electrons in the low energy level degenerate 1π orbitals greatly strengthens the Si−O bond, but almost does not give any effect on the Si−C bond. On the other hand, the occupation of two electrons in the degenerate HOMO (2π) will strengthen the Si−C bond and reduce the Si−O bond. Because the 2π orbitals are energetically higher than the 1π orbitals, the effect of 2π on the C−Si−O skeleton bond is greater than that of 1π. The modification to 1π bonding by 2π orbitals results in that the Si−O bond is slightly weakened and the Si−C bond is strengthened. Therefore, the overall effect of several kinds of bonding orbitals exhibits that there are two kinds of bonding (σ, π) between Si and O and between Si and C centers, respectively, but the Si−O bond is stronger than the Si−C bond.

As mentioned above, although the charge population is not comparable between two linear species, the linear SiCO and the linear CSiO, their structural formalism is similar. It may also be demonstrated by the bonding analysis and the orbital interaction character. Comparison of the interaction character of the corresponding MO between the linear SiCO and the linear CSiO (comparing Figure 1a with Figure 1d) indicates that the four σ orbitals (1σ, 2σ, 3σ, 4σ) and two π orbitals (1π, 2π) of the linear SiCO molecule are equivalent in nature to those of the linear CSiO molecule except for the exchange of the positions of Si and C atoms. This may be understandable because Si and C belong to the same group in the periodic table and should have same bonding character. From this, it can be concluded that the linear SiCO and the linear CSiO species should be classified as the analogue only with a minor difference that the C−SiO bond is slightly stronger than the Si−CO bond, and the corresponding C−SiO bond length is slightly longer than the Si−CO bond length.

The same conclusion can be drawn by the frequency analysis. For the three vibrational modes of the linear CSiO species in both states, ω_2 is the bending vibrational mode departing from the linearity, whereas ω_3 is referred to the stretching vibration of the C−SiO bond, and ω_1 is that of the CSi−O bond. The very small bending vibrational frequencies imply that the bending PES is very flat, and the corresponding isomerization barrier is low, and the molecule is facile. The possibility of the isomerization of the linear CsiO species is that the $^3\Sigma^-$ state is greater than the $^1\Delta$ state. To the best of our knowledge, there are no experimental or theoretical investigations on the $^1\Delta$ state and the other singlet states of the linear CSiO molecule. For the mode ω_3, it reflects C−SiO bond stretching vibrational strength. The frequencies in the $^3\Sigma^-$ state are slightly smaller

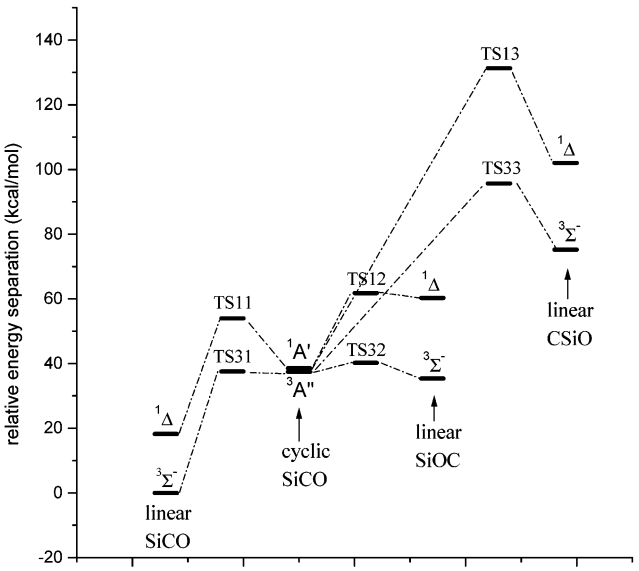

Figure 2. State−state correlation diagram.

by 35 cm^{-1} than those of $^1\Delta$ state at the CASSCF/6-311+G* level. They are significantly smaller than those ($^3\Sigma^-$, 859.2 cm^{-1} and $^1\Delta$, 829.9 cm^{-1}) of the free state SiC moiety. This indicates that the C−SiO bond is weaker than the free state Si−C bond, exhibiting different bonding character. Similarly, for the Si−O vibration ω_1, the frequency in the $^3\Sigma^-$ state is almost equal to that in the $^1\Delta$ state (only greater by 8 cm^{-1} than the $^1\Delta$ state). They are very close to that of the free state SiO. This phenomenon has implied that in the formed C−SiO linear molecule the Si−O moiety still keeps the character of the free state SiO molecule and the combination with C does not obviously change Si−O bond strength.

4. Isomerization Mechanism

To find the correlations among all states mentioned above, the transition state structure searches have been carried out at the B3LYP/6-311+G* level, and the corresponding state−state geometrical isomerization pathways have also been performed by using the intrinsic reaction coordinate method and have also been confirmed by scanning the relaxed PES against ∠CSiO. The transition energies have been calibrated at the CASSCF/6-311+G* level by using B3LYP/6-311+G* geometries. The state-state correlations are described in Figure 2. From Figure 2, it can be known that there are three possible transition states for the triplet state isomers, and the same is true for the singlet state isomers. No direct transition states are found for the other three isomerization pathways in both states: the linear SiCO → the linear SiOC, the linear SiCO → the linear CSiO, and the linear SiOC → the linear CSiO. Actually, any two linear states are also correlative perhaps by a cyclic stable isomer, being referred to as an intermediate. All of the transition state structural parameters have been given in Table 5. The activation energies of these isomerizations may be extracted from the corresponding ΔE given in Tables 3−5. For the linear SiCO isomer, although it cannot directly correlate to the linear SiOC and the linear CSiO isomers, it may isomerize into the linear SiOC and CSiO by undergoing two transition states and one intermediate. Because of no correlation between the triplet state and the singlet state isomers, the discussions will focus on the isomerizations among the isomers with the same spin state.

For the triplet state, the ground state SiCO has only one isomerization pathway, viz., it may change into the cyclic SiCO isomer by surmounting a barrier of 37.6 kcal/mol. However,

its inverse pathway is very easy; the activation barrier is ~0.1 kcal/mol at B3LYP/6-311+G* level. The first step for the isomerization from the linear SiCO to the cyclic SiCO is the bending of the linear SiCO configuration. Because the bending has broken one of two degenerate π bonds, the Si−C bond is getting weak long along with the decrease of the ∠SiCO angle. When the ∠SiCO angle becomes 94.1°, the system reaches the transition state. The optimized geometric parameters of the transition state (TS31) are 2.296 Å/Si−C, 2.641 Å/Si−O, and 1.154 Å/C−O, respectively. The TS31 is geometrically very close to the cyclic SiCO isomer (2.124 Å/Si−C, 2.467 Å/Si−O, and 1.172 Å), especially for the ∠SiCO angle 94.1°. Together with the calculated charge population and the spin density distribution, these geometrical parameters have indicated that TS31 may be certainly assigned to the transition state for the isomerization between the linear SiCO (the ground state) and the cyclic SiCO isomers. The further IRC pathway analysis has also confirmed this assignment. After surmounting TS31, the system goes to a stable cyclic structure along a flat IRC PES. From the cyclic SiCO isomer, there are two possible isomerization pathways for the further development, going to the linear SiOC or the linear CSiO species, respectively. Of two further isomerization pathways, the easier one is to go to the linear SiOC species. This pathway has a very small barrier being 2.74 kcal/mol for the cyclic SiCO → TS32 process and 4.88 kcal/mol for the linear TS32 ← SiOC process. These three states (the initial state, the transition state, and the final state) are almost energetically equivalent. The transition state search has indicated that it is very difficult to find TS32 at the B3LYP/6-311+G* level. Even if basis set is changed, the B3LYP method still does not locate TS32. Fortunately, the B3P86 method can easily give the TS32 configuration. The optimized bond length parameters are 3.304 Å for Si−C, 3.035 Å for Si−O, and 1.130 Å for C−O bond. Obviously, TS32 keeps the cyclic feature, and the key angle ∠SiOC is 93.6° and is close to that (ca. 60°) of the cyclic SiCO and apart from that (180°) of the linear SiOC, but the Si−O and C−O bonds have tended to those of the linear SiOC isomer. The charge population and the spin density distribution are also close to the linear isomer. Inspection of the only imaginary frequency mode indicates that the vibration is directed to both of the cyclic SiCO and the linear SiOC isomers. However, this mode has a very small frequency value, and the vibrational PES for the isomerization according to this mode is flat, the barrier is low, and thus the nuclear tunneling effect is small. Another isomerization pathway starting from the cyclic intermediate is to go to the linear CSiO species by experiencing TS33. In this pathway, there is the rupture of the C−O bond, which results in the strengthening of the Si−C and Si−O bonds. Obviously, this isomerization is more difficult than the TS32 mechanism, because it must surmount a high barrier (58.02kcal/mol) mainly attributed to the rupture of the C−O bond. The optimized TS33 geometrical parameters are 1.935 Å for the Si−C bond and 1.562 Å for the Si−O bond, and they are slightly longer than those of the linear CSiO species. The C−O bond (2.599 Å) and the corresponding ∠CSiO angle (95.4°) are significantly greater than those (1.173 Å and 28.3°) of the cyclic species. These data indicate that the C−O bond has been broken before the transition state (TS33). After TS33, the system is relaxed by strengthening the Si−O and Si−C bonds, and the corresponding energy change, viz., the backward activation energy, is about 20.5 kcal/mol. Inspection of the only imaginary frequency mode indicates that its frequency value is 625.2 cm^{-1}, being much greater than those of the other two imaginary frequency modes. Together with high activation barrier, it can be predicted that there is great nuclear tunneling effect in this TS33 mechanism. Obviously, this cyclic SiCO → TS33 → linear CSiO mechanism is an endothermic process and is of the thermodynamic control, whereas the cyclic SiCO → TS32 → linear SiOC mechanism is a weakly exothermic process with a low barrier and is of the kinetic control. In short word, the TS32 pathway is much easier than the TS33 one.

Although no transition state for the direct correlation of the linear SiOC with the linear CSiO species has been found, they may interchange by experiencing another pathway including two transition states and one intermediate. For an example of the isomerization from the linear SiOC to linear CSiO species, first, the linear SiOC is bent to be TS32 by absorbing 4.88 kcal/mol (activation energy) and then changes to the cyclic SiCO intermediate. Second, the system reaches the linear CSiO by undergoing TS33, as mentioned above. Therefore, it can be claimed that there is essentially a correlation among four triplet state isomers; three linear isomers do not directly correlate to each other by an one-step mechanism, but they may do so by a two-step mechanism including two transition states and one intermediate. Of particular interest for the cyclic isomer is that the respective breakings of three bonds (Si−C, Si−O, and C−O) has explicitly implied three different isomerization directions. The easiest one is to break the Si−O bond and to go to the ground state (the linear SiCO species) by experiencing TS31, but its inverse process is more difficult. The most difficult process is to break the C−O bond and to go to the linear CSiO.

Similar analysis may be made for the singlet state processes. From Figure 2, it can be known that there is the same correlation and same isomerization mechanism among the singlet state isomers as those among the triplet state isomers. The singlet state linear SiCO may isomerize into the cyclic SiCO by undergoing TS11, and the corresponding forward and backward activation energies are 35.79 and 15.49 kcal/mol, respectively. The optimized TS11 parameters are 2.414 Å/Si−C, 2.425 Å/Si−O, 1.157 Å/C−O, and 75.6°/∠SiCO, respectively. They are slightly different from the similar triplet state structures with an exception of the C−O bond length. In particular, the bend angle ∠SiCO is smaller by ca. 18° than that of TS31. The forward activation barrier is very close to that of the corresponding triplet state pathway, but the activation barrier of its inverse process is greater by ca. 15 kcal/mol than that of the triplet state. The imaginary frequency is also greater than that of TS31, indicating that the nuclear tunneling effect is slightly larger than that in the triplet state. From the cyclic $^1A'$ state, there are also two pathways for the further development. For TS12, the forward activation energy is 23.3 kcal/mol and is obviously greater than that (2.74 kcal/mol) of TS32, but the backward one is 1.51 kcal/mol, being slightly smaller than that (4.88 kcal/mol) of TS32. The optimized TS12 structural parameters indicate that there will be large structural changes if the electronic state is excited from the triplet to the singlet states or inverse. Obviously, this phenomenon should be attributed to the same electron occupation mode as those in the linear SiOC and the cyclic SiCO isomers. For the triplet state, the $^3\Sigma$ originates from the $\pi_+^1\pi_-^1$ occupation, and the $^3A''$ state originates from the $\pi^1\pi'^1$ occupation. In the later, the π' orbital is actually referred to 6*a*′ in Figure 1b (the cyclic SiCO isomer), and it is the linear combination of the in-plane p orbital of Si and the in-plane π^* of CO by another interaction formalism instead of linearly conjugated π bond. The HOMO electronic configuration of TS12 is $\pi^1\pi''^1$, and the interaction formalism of π'' is similar to π' with different coupling amplitude. When

the triplet state is excited to the singlet state, the corresponding electronic configurations change into $\pi_+0\pi_-2$ ($^1\Delta$), $\pi^0\pi'^2$ ($^1A'$), and $\pi^0\pi''^2$ (TS12). Comparison of the HOMO bonding nature between the triplet state and the singlet state has shown that there is not a major difference in the coupling formalism between two different spin states; thus, TS12 and TS32 are structurally similar.

For the isomerization from the cyclic species to the linear CSiO species via a singlet state mechanism, there is a highest barrier transition state with 92.78 kcal/mol of the forward activation energy and 29.25 kcal/mol of backward activation energy, compared with other two kinds of the transition states. The optimized geometrical parameters of TS13 are very close to those of TS33, but the activation barriers of the singlet state pathway are far greater than those of the triplet state pathway. This may be explained in terms of the bonding character of the two cyclic isomers. As mentioned above, the HOMO electronic configurations are $(6a')^1(2a'')^1$ for $^3A''$ and $(6a')^2(2a'')^0$ for $^1A'$. After the cyclic SiCO isomerizes into the linear CSiO species, its two key orbitals ($6a'$ and $2a''$) change into two degenerate π orbitals (2π of the linear CSiO species in Figure 1d). For the out-of-plane orbital (π-type), there is not large overlap integral change in the process of $2a'' \rightarrow 2\pi$ (out-of-plane). However, for the in-plane orbital, the overlap integrals are significantly different in $6a' \rightarrow 2\pi$ (in-plane) process. In the cyclic SiCO species, $6a'$ may be considered as the interaction between the in-plane Si p_z orbital and the π_y* antibonding orbital (cf. Figure 1b). Along with the increase of ∠CSiO angle, the C−O bond is getting to be weakened and to become ruptured. The in-plane π_y* orbital becomes two separate p_y orbitals. In parallel, the coupling of Si p_z with the p_y of C and O centers becomes unfavorable, whereas the effective coupling of the Si p_y orbital with the p_y of C and O atoms is gradually increased. The overall coupling interaction between Si ($p_z + p_y$) and p_y orbitals of C and O behaves as curve-type dependence on ∠CSiO angle with a minimum. This minimum coupling corresponds to the position where C and O atoms are situated at two interfaces between p_z and p_y of the Si atom, respectively. The corresponding energy level of the MO formed by this coupling should be the highest, and from the viewpoint of total energy, the system also should be energetically the highest if this orbital is occupied. Namely, in the process of the isomerization, along with the increase of ∠CSiO angle, the system (CSiO) behaves as the parabola-like energy relationship. The top of the parabola corresponds to the transition state. Therefore, for the isomerization of the cyclic SiCO to the linear CSiO, it is understandable that there are higher activation barriers than the other mechanism. In particular for the singlet state mechanism, two electrons occupy this kind of orbital ($6a'$), the activation barrier is certainly greater than that of the triplet state pathway in which only one electron occupies this kind of orbital. Because the minimum coupling between Si and (C, O) occurs at the two interfaces between p_z and p_y orbitals of the Si center, and the angle between these two interfaces is 90°, the angle ∠CSiO at the transition state should be about 90°. Our optimized ∠CSiO angle in both states are 94∼95° at the B3LYP/6-311+G* level, having confirmed the above prediction.

5. Conclusion

The structural properties for the subcarbonyl Si, SiCO, and its isomers in the singlet and triplet states have been investigated using CASSCF, three DFT, and MP2 methods with a 6-311+G* basis set. The detailed bonding character has been discussed. Results indicate that there are four different isomers for each state (one cyclic SiCO and three linear: SiCO, SiOC, and CSiO species), and for each geometrical configuration, the triplet state is more stable than the corresponding singlet state. The most stable one is the linear SiCO species in the triplet state ($^3\Sigma^-$) and may be referred to the global minimum. At the CASSCF-MP2(full)/6-311+G* level, the state−state energy separations of the other triplet states relative to the ground state are 43.2 (cyclic), 45.2 (linear SiOC), and 75.6 kcal/mol (linear CSiO), respectively, whereas the triplet−singlet state excitation energies for each configuration are 17.3 (linear SiCO), 2.2 (cyclic SiCO), 10.2 (linear SiOC), and 18.5 kcal/mol (linear CSiO), respectively. For the linear SiCO isomers, the combination of Si with CO yields a weak Si−CO bonding and simultaneously reduces the C−O bonding. The formed SiCO ($^3\Sigma^-$) may be classified as silene (carbonylsilene), and its $CO^{\delta-}$ moiety possesses CO^- property. Although the Si−C bond length is similar to the single bond, the bond strength is weaker than the common Si−C bonds in the silicon-containing alkane. Using the CASSCF/6-311+G* method, the calculated dissociation energy is 42.5 kcal/mol, whereas the calculated vertical IP is 188.8 kcal/mol, being very close to the first IP of Si atom.

Another two linear isomers (SiOC and CSiO) have similar structural bonding character to that of the linear SiCO species, and SiOC may be referred to the iso-carbonyl Si instead of the aether compound, whereas the CSiO isomer may be considered as the combination of C (the analogue of Si) with SiO (the analogue of CO). The bonding, no matter the singlet or triplet states, is weak for these linear species, and the corresponding PESs are flat at the equilibrium positions; therefore, these linear molecules are facile. Another important isomer is of cyclic structure, it may be considered as the combination of CO with Si by the side π bond. This structure has the smallest $^3A''-^1A'$ state excitation energy (∼2.2 kcal/mol), the C−O bonds are longer, and the corresponding vibrational frequencies are significantly smaller than those of the other linear species. These cyclic species also are not classified as epoxy compounds. State−state correlation analysis and the isomerization pathway searches have indicated that there are no direct correlations among three linear structures at each spin state, but they may interchange by experiencing two transition states and one cyclic intermediate. In other words, the respective breakings of the three bonds (Si−C, Si−O, and C−O) of the cyclic species denote three different isomerization directions. The easiest pathway is to break the Si−O bond to go to the linear SiCO, but its inverse process is very difficult. The most difficult process is to break the C−O bond and to go to the linear CSiO.

In addition, it should be noted that because of the importance of investigations regarding the weak interaction in biological and materials fields, the detailed studies about not only the interaction among large molecules but also that between large and small molecules need paying a further attention. Perhaps investigations on the interaction and bonding among such small molecules may provide some valuable information.

Acknowledgment. This work is supported by (NKBRSF) and NSFC (29973022) and Foundation for Key Teachers in University of State Ministry of Education of China. The author (Y.B.) is also very thankful to the referees for their many helpful comments.

References and Notes

(1) Ray, G. B.; Li, X.-Y.; Ibers, J. A.; Sessler, J. L.; Spiro, T. G. *J. Am. Chem. Soc.* **1994**, *116*, 162.

(2) Alben, J. O.; Caughey, W. S. *Biochemistry* **1967**, *17*, 175.

(3) Collman, J. P.; Brauman, J. I.; Halbert, T. R.; Suslick, K. S. *Proc. Natl. Acad. Sci. U.S.A.* **1976**, *73*, 3333.
(4) Li, X.-Y.; Spiro, T. G. *J. Am. Chem. Soc*. **1988**, *110*, 6024.
(5) Ramsden, J.; Spiro, T. G. *Biochemistry* **1989**, *28*, 3125.
(6) Barlow, C. H.; Ohlsson, P.-I.; Paul, K.-G. *Biochemistry* **1976**, *15*, 2225.
(7) Yoshikawa, S.; Choc, M. G.; O'Toole, M. C.; Caughey, W. S. *J. Biol. Chem.* **1977**, *252*, 5498.
(8) Jewsbury, P.; Kitagawa, T. *Biophys. J.* **1994**, *67*, 2236.
(9) Springer, B. S.; Sligar, S. G.; Olson, J. S.; Phillips, G. N., Jr. *Chem. Rev*. **1994**, *94*, 699.
(10) Staemmler, V. *Chem. Phys*. **1975**, *7*, 17.
(11) Ikuta, S. *Chem. Phys. Lett.* **1984**, *109*, 550.
(12) Del Bene, J. E. *J. Comput. Chem*. **1986**, *7*, 259.
(13) Walter, D.; Sievers, M. R.; Armentrout, P. B. *J. Mass. Spectrosc. Ion Proc*. **1998**, *175*, 93.
(14) Alikani, M. E.; Bouteiller, Y. *J. Mol. Struct.* **1997**, *436*, 481.
(15) Alikani, M. E. *J. Mol. Struct.* (*THEOCHEM*) **1998**, *432*, 263.
(16) Pullumbi, P.; Bouteiller, Y.; Perchard, J. P. *J. Chem. Phys*. **1995**, *102*, 5719.
(17) Pullumbi, P.; Bouteiller, Y. *Chem. Phys. Lett.* **1995**, *234*, 107.
(18) Wesolowski, S. S.; Galbraith, J. M.; Schaefer, H. F., III. *J. Chem. Phys*. **1998**, *108*, 9398.
(19) Balaji, V.; Sunil, K. K.; Jordan, K. D. *Chem. Phys. Lett.* **1987**, *136*, 309.
(20) Wesolowiski, S. S.; Crawford, T. D.; Ferman, J. T.; Schaefer, H. F., III. *J. Chem. Phys.* **1996**, *104*, 3672.
(21) Zhang, L.; Dong, J.; Zhou, M. *Chem. Phys. Lett.* **2001**, *335*, 334.
(22) Zhang, L.; Dong, J.; Zhou, M. *J. Chem. Phys.* **2000**, *113*, 8700.
(23) Burkholder, T. R.; Andrews, L. *J. Phys. Chem*. **1992**, *96*, 10195.
(24) Riemer, W. H.; Zika, R. G. *Marine Chem*. **1998**, *62*, 89.
(25) Goldman, A.; Coffey, M. T.; Stephen, T. M.; Rinsland, C. P.; Mankin, W. G.; Hannigan, J. W. *J. Quant. Spectrosc. Radiat. Transfer* **2000**, *67*, 447.
(26) Jacox, M. E.; Milligan, D. E.; Moll, N. G.; Thompson, W. E. *J. Chem. Phys*. **1965**, *43*, 3734.
(27) Devillers, M. C. *Compt. Rend. Acad. Sci.* **1966**, *262c*, 1485.
(28) Lembke, R. R.; Ferrante, R. F.; Weltner, W., Jr. *J. Am. Chem. Soc.* **1977**, *99*, 416.
(29) Stolvik, R. *J. Mol. Struct*. **1985**, *124*, 133.
(30) Petraco, N. D. K.; Brown, S. T.; Yamaguchi, Y.; Schaefer, H. F., III. *J. Phys. Chem. A* **2000**, *104*, 10165.
(31) Dekook, R. L.; Grev, R. S.; Schaefer, H. F., III. *J. Chem. Phys.* **1988**, *89*, 3016.
(32) Grev, R. S.; Schaefer, H. F., III. *J. Am. Chem. Soc*. **1989**, *111*, 5687.
(33) Petraco, N. D. K.; Brown, S. T.; Yamaguchi, Y.; Schaefer, H. F., III. *J. Chem. Phys.* **2000**, *112*, 3201.
(34) Archibong, E. F.; St-Amant, A. *Chem. Phys. Lett*. **1998**, *284*, 331.
(35) Bu, Y.; Song, X. *J. Chem. Phys*. **2000**, *113*, 4216.
(36) Bu, Y. *Chem. Phys. Lett.* **2000**, *322*, 503.
(37) Bu, Y.; Song, X.; Liu, C. *Chem. Phys. Lett.* **2000**, *319*, 725.
(38) Bu, Y. *Chem. Phys*. **2001**, *271*, 229; *ibid* **2001**, *273*, 103.
(39) Bu, Y. *Chem. Phys. Lett.* **2001**, *338*, 142.
(40) Frisch, M. J.; Trucks, G. W.; Schlegel, H. B.; Gill, P. M. W.; Johnson, B. G.; Robb, M. A.; Cheeseman, J. R.; Keith, T.; Petersson, G. A.; Montgomery, J. A.; Raghavachari, K.; Al-Laham, M. A.; Zakrzewski, V. G.; Ortiz, J. V.; Foresman, J. B.; Peng, C. Y.; Ayala, P. Y.; Chen, W.; Wong, M. W.; Andres, J. L.; Replogle, E. S.; Gomperts, R.; Martin, R. L.; Fox, D. J.; Binkley, J. S.; Defrees, D. J.; Baker, J.; Stewart, J. P.; Head-Gordon, M.; Gonzalez, C.; Pople, J. A. *Gaussian 94*, revision B.2; Gaussian, Inc.: Pittsburgh, PA, 1995.
(41) Becke, A. D. *J. Chem. Phys.* **1993**, *98*, 5648.
(42) Lee, C.; Yang, W.; Parr, R. G. *Phys. Rev. B* **1988**, *37*, 785.
(43) Stephens, P. J.; Devlin, F. J.; Ashvar, C. S.; Chabalowki, C. F.; Frish, M. J. *Faraday Discuss.* **1994**, *99*, 103.
(44) Perdew, J. P. *Phys. Rev. B* **1986**, *33*, 8822.
(45) Perdew, J. P. *Phys. Rev. B* **1986**, *34*, 7406.
(46) Perdew, J. P.; Wang, Y. *Phys. Rev. B* **1992**, *45*, 13244.
(47) Cai, Z. L.; Wang, Y. F.; Xiao, M. H. *Chem. Phys. Lett.* **1992**, *191*, 533.
(48) Hoffmann, R. *J. Am. Chem. Soc.* **1983**, *105*, 1084.
(49) Lee, T. J.; Fox, D. J.; Schaefer, H. F., III.; Pitzer, R. M. *J. Chem. Phys.* **1984**, *81*, 356.